

## Combined lattice-location-hyperfine-interaction experiments on Hg implanted in Fe

P. K. James, P. Herzog,\* and N. J. Stone

*Mullard Cryomagnetic Laboratory, Clarendon Laboratory, Oxford, England*

K. Freitag

*Institut für Strahlen-und Kernphysik der Universität Bonn, Bonn, Germany*

(Received 1 May 1975; revised manuscript received 25 August 1975)

The channeling technique has been used to study the lattice location of Hg implanted at 80 keV into Fe. The impurity is found to be almost entirely substitutional at a dose of  $5 \times 10^{14}$  ions  $\text{cm}^{-2}$ . Using implanted sources nuclear magnetic resonance of oriented nuclei (NMR/ON) was observed both for  $Fe^{203}\text{Hg}$  and  $Fe^{197}\text{Hg}^m$ . The  $Fe^{203}\text{Hg}$  resonance observed in an external field of 2.1 kG at 216.4(2) MHz gives  $B_{\text{hf}}(Fe\text{Hg}) = -838.1(8)$  kG. For  $Fe^{197}\text{Hg}^m$  the resonance at 100.9(1) MHz in an applied field of 2.3 kG yields  $B_{\text{hf}}(Fe\text{Hg}) = -839.5(8)$  kG. Both experiments were performed at temperatures below 1 K. The values of  $B_{\text{hf}}(Fe\text{Hg})$  found in the literature are compared with these values. The difference between the results of time-differential perturbed-angular-correlation experiments at room temperature and the result of the present NMR/ON investigation is ascribed to a temperature anomaly. The hyperfine anomaly  $\Delta(^{197}\text{Hg}^m-^{203}\text{Hg}) = +0.17(14)\%$  has been derived. The spin-lattice relaxation times of  $^{203}\text{Hg}$  and  $^{197}\text{Hg}^m$  in iron are  $T_1 = 61(7)$  sec and  $T_1 = 190(40)$  sec, respectively, at 20 mK.

### I. INTRODUCTION

The hyperfine field of mercury in iron has been studied extensively.<sup>1-7</sup> Several techniques and different isotopes have been used for these investigations. The results are summarized in Table I. A spread between 440 and 640 kG exists in results obtained using the technique of integral perturbed angular correlation (IPAC) as applied to the 412-keV  $2^+$  state of  $^{198}\text{Hg}$  (Refs. 1-4 and 7). The results of time-differential perturbed-angular-correlation (TDPAC) experiments, which are less liable to systematic errors, are in good internal agreement. They were done at room temperature observing the Larmor precession of the 158-keV state in  $^{199}\text{Hg}$  (Ref. 5) and of the 134-keV state of

$^{197}\text{Hg}$  (Ref. 6). The average field from both experiments is 680(40) kG, where the error is almost entirely due to uncertainties in the nuclear  $g$  factors.

The present work was undertaken to resolve the differences between these results, and to improve the precision of the field determination by the application of a third technique, nuclear magnetic resonance of oriented nuclei (NMR/ON). Since NMR/ON sources of  $Fe/Hg$  can only be prepared by ion implantation, with the resulting problems associated with the location of the implanted ions, a channeling experiment using Rutherford back-scattering was performed to locate the implanted Hg atoms. This is described in Sec. II.

Initially,  $^{203}\text{Hg}$  was chosen as a suitable isotope,

TABLE I. Hyperfine field of mercury in iron measured by different techniques.

Isotope	Technique	Source preparation	Temperature (K)	$B_{\text{hf}}$ (kG)	Reference
$^{198}\text{Hg}$	IPAC	thermal, $FeAu$	295	-630(160)	1 <sup>a</sup>
$^{198}\text{Hg}$	IPAC	thermal, $FeAu$	295	-490(125)	2
$^{198}\text{Hg}$	IPAC	thermal, $FeAu$	295	-440(105)	3
$^{198}\text{Hg}$	IPAC	thermal and implanted, $FeAu$	295	-640 (160)	4
$^{199}\text{Hg}$	TDPAC	implanted, $FeTl$	295	-670(65) <sup>b</sup>	5
$^{197}\text{Hg}$	TDPAC	implanted, $FeHg$	295	-692(55)	6
$^{198}\text{Hg}$	IPAC	thermal, $FeAu$	295	-590(160)	7
$^{203}\text{Hg}$	NMR/ON	implanted, $FeHg$	< 1	-838.1(8)	this work
$^{197}\text{Hg}$	NMR/ON	implanted, $FeHg$	< 1	-839.5(8)	this work

<sup>a</sup>Value from Ref. 1 revised as cited in Ref. 4.

<sup>b</sup>Field at the site of the majority of nuclei.

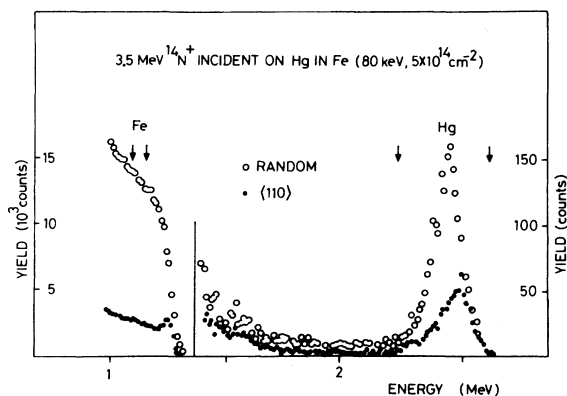


FIG. 1. Backscattered energy spectra for 3.5-MeV  $^{14}\text{N}^+$  ions incident in  $\langle 110 \rangle$  and random directions in an Fe single crystal implanted with Hg. In the high-energy region the vertical scale has been expanded. The integrated target current was the same in both cases.

having a conveniently long half-life of 47 days, a well-known magnetic dipole moment  $\mu = 0.84895(13)$  (Ref. 8 corrected for diamagnetic shielding), and a simple decay scheme [see Fig. 3(a)]. Work on this isotope is described in Sec. III.

The result of the  $Fe^{203}\text{Hg}$  NMR/ON study,  $B_{\text{hf}} = -838.1(8)$  kG, differed so markedly from all previous work that it was necessary to check whether this could be caused by a  $g$  factor error or by systematic differences between different implantation techniques. Accordingly, a second NMR/ON experiment was made using the same  $^{197}\text{Hg}$  activity as had been used in one of the TDPAC studies,<sup>6</sup> with the same implantation conditions as in that work. This work is described in Sec. IV. The results are summarized and discussed in Sec. V.

## II. CHANNELING ON IMPLANTED MERCURY IN IRON

### A. Samples

The location experiments were performed on an Fe single crystal, obtained from Materials Research Company Ltd., in the form of a cylindrical rod. The purity of the Fe was 99.92%, the crystal having been grown by the strain-anneal technique. The rod was oriented using x-ray diffraction and then spark cut into 1-mm-thick disks, perpendicular to the  $\langle 110 \rangle$  axis. The crystals were spark planed and then electropolished in an electrolyte consisting of 7% perchloric acid and 93% glacial acetic acid.<sup>9</sup>

The inactive  $^{202}\text{Hg}$  implant was performed at room temperature on the Harwell Mk IV separator at 80 keV with a dose of  $5 \times 10^{14}$  ions  $\text{cm}^{-2}$ . In order to minimize channeling effects during implantation, the crystal was tilted so that the  $\langle 110 \rangle$  axis was  $\sim 7^\circ$  from the beam direction. The projected range of the ions was 210 Å with a standard

deviation of 60 Å so that the average local concentration of Hg atoms in the implanted region was 0.4 at. %.

### B. Backscattering experiment

The channeling experiment was performed on the Harwell 5MV Van de Graaff channeling facility.<sup>10</sup> The beam was collimated to a diameter of 1 mm and an angular divergence of  $\pm 0.03^\circ$ . Crystal alignment was carried out with 3.0-MeV  $^4\text{He}$  ions using a goniometer which allowed the target to be rotated about three independent axes<sup>11</sup> in steps of  $0.01^\circ$ . In addition, the goniometer has been provided with a fourth motion which moves the target laterally perpendicular to the beam. Thus, after alignment the crystal can be moved so that the beam impinges on a fresh spot. Backscattered particles were detected at  $165^\circ$  by a 50-mm<sup>2</sup> ORTEC Si surface-barrier detector at 7 cms from the target. Care was taken to avoid blocking effects for the scattered particles.

Figure 1 shows the backscattering energy spectra for 3.5-MeV  $^{14}\text{N}$  ions incident in  $\langle 110 \rangle$  and random directions, both for an integrated target charge of 1.8  $\mu\text{C}$ . The Fe and Hg windows are also shown, the Fe window being chosen to correspond to the depth of the Hg implant. The Hg yields were corrected for background, this correction being small as the Hg peak lies above the limit of Fe pile up. Spectra were accumulated at various angles and at beam currents between 0.5 and 1.5 nA in order to maintain the analyzer dead-time constant at 2%. Integrated charges of 1.8  $\mu\text{C}$  were used in all cases.

Complete angular scans were made for the  $\langle 110 \rangle$  axis and the  $\langle 211 \rangle$  plane; in addition,  $\chi_0$  (minimum-yield) measurements were made for the  $\langle 111 \rangle$  axis and the  $\langle 100 \rangle$  and  $\langle 110 \rangle$  planes. The existence of flux peaking<sup>12</sup> means that a particular value of  $\chi_0$  can correspond to several different distributions of impurity atoms, hence the need to carry out detailed angular scans.

Figure 2 shows the  $\langle 110 \rangle$  axial and  $\langle 211 \rangle$  planar scans. The angular widths of the Hg scans are the same as those of Fe in both cases and the minimum yields are similar. Of particular importance is the absence of structure in the Hg yield. The results of all  $\chi_0$  measurements made are listed in Table II; again there is close agreement between the Hg and Fe yields. Thus, the majority of Hg atoms would appear to occupy substitutional sites.

Using a simple model whereby Hg atoms are either substitutional or totally random (their yield is approximately independent of angle) the results indicate an average of  $(92 \pm 5)\%$  substitutional. Because of the large proportion of Hg atoms substitutional in the  $5 \times 10^{14}$  ion  $\text{cm}^{-2}$  sample, backscattering experiments were not performed on a

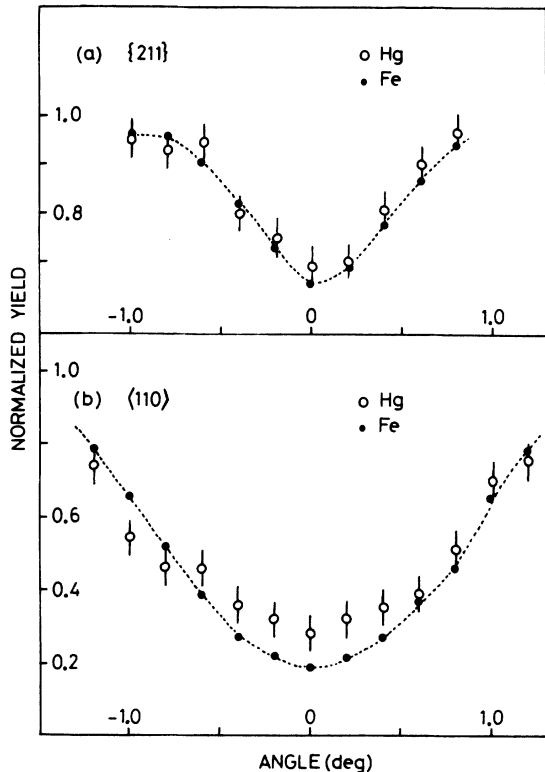


FIG. 2. Backscattering yields normalized to the random values for Hg implanted in Fe. Showing the yield as a function of angle (a) near a {211} plane and (b) near a  $\langle 110 \rangle$  axis. The dotted lines through the Fe points are only to guide the eye.

$1 \times 10^{14}$  ion  $\text{cm}^{-2}$  sample (the maximum dose used in the hyperfine-interaction experiments) as decreasing dose would be unlikely to give a very different substitutional percentage.

### III. HYPERFINE-INTERACTION MEASUREMENTS ON $Fe^{203}Hg$

#### A. Source preparation

Two iron samples were prepared for implantation, one cut from the same single crystal as was used for the location work, the other a  $75\text{-}\mu\text{m}$  foil from Koch-Light Ltd. and assayed as 99.999% pure. Both were electropolished (as in Sec. II A) and then soft soldered to copper tags.  $^{203}Hg$  was obtained from the Radiochemical Centre, Amersham, Bucks., in the form of mercuric chloride in aqueous solution, its specific activity being 0.7 mCi/mg. After self-plating the mercury onto copper wires it was ready for implantation. The implants were performed at room temperature on the Harwell Mk I separator at 80 keV. The dose in both cases was  $(1.2 \pm 0.3) \times 10^{14}$  ions  $\text{cm}^{-2}$ . The uncertainty in the dose arises from the use of post acceleration on the Mk I machines. After implantation the sources were stored at liquid-nitrogen tempera-

tures until required.

#### B. Nuclear orientation of $Fe^{203}Hg$

A thermal-equilibrium-nuclear-orientation experiment measures the angular distribution of radiation emitted from radioactive nuclei embedded in suitable hosts as a function of temperature. For  $\gamma$  rays the observed distribution is described by

$$W(\theta) = \sum_{\nu=0, \nu \text{ even}} B_{\nu} \left( \frac{\mu B}{IkT}, I \right) U_{\nu} F_{\nu} P_{\nu}(\cos\theta) Q_{\nu}, \quad (1)$$

where  $I$  is the parent nuclear spin.  $P_{\nu}$  is a Legendre polynomial,  $U_{\nu}$  and  $F_{\nu}$  are the preceding and observed decay parameters,<sup>13</sup> and the  $Q_{\nu}$ 's allow for the finite solid angle of the detector. In the case of the 279-keV  $\gamma$  ray of  $^{203}Hg$ , all these parameters are relatively well known so that a nuclear-orientation experiment will give information about the orientation parameter  $B_{\nu}$ . Nuclear orientation is an integral technique and so is generally only able to measure an average field. This poses problems in the case of implanted sources, as impurities may reside in a variety of positions in the lattice. However, if the nuclear-orientation results can be combined with those of an NMR experiment, information can be obtained about the proportion of impurities in good sites as well as the hyperfine field itself.

The nuclear-orientation experiments were performed on the apparatus described in Ref. 14. The copper tag holding the polycrystalline  $Fe^{203}Hg$  sample was soldered to the cold finger of a chrome-alum salt pill using Wood's metal; during this process the Fe sample itself was immersed in liquid nitrogen. In addition, a  $Fe^{60}Co$  thermometer was also soldered to the copper tag.

The salt pill was cooled to 13 mK, the sample polarized in an external field of 5.3 kG, and the  $\gamma$ -ray spectrum from a Ge(Li) detector accumulated for 15-min intervals over 4 h as the salt pill returned slowly to 1 K. The resultant temperature-dependent anisotropy of the 279-keV  $\gamma$  ray is shown

TABLE II. Aligned to random yields for backscattering of 3.5-MeV  $^{14}N$  from Fe and Hg in various channeling directions for implanted  $5 \times 10^{14}\text{-cm}^{-2}$  80-keV  $FeHg$ .

Channel	$\chi_0(Fe)$	$\chi_0(Hg)$
$\langle 110 \rangle$	0.19	$0.28 \pm 0.05$
$\langle 111 \rangle$	0.10	$0.27 \pm 0.15$
{100}	0.69	$0.74 \pm 0.04$
{110}	0.46	$0.39 \pm 0.06$
{211}	0.65	$0.68 \pm 0.04$

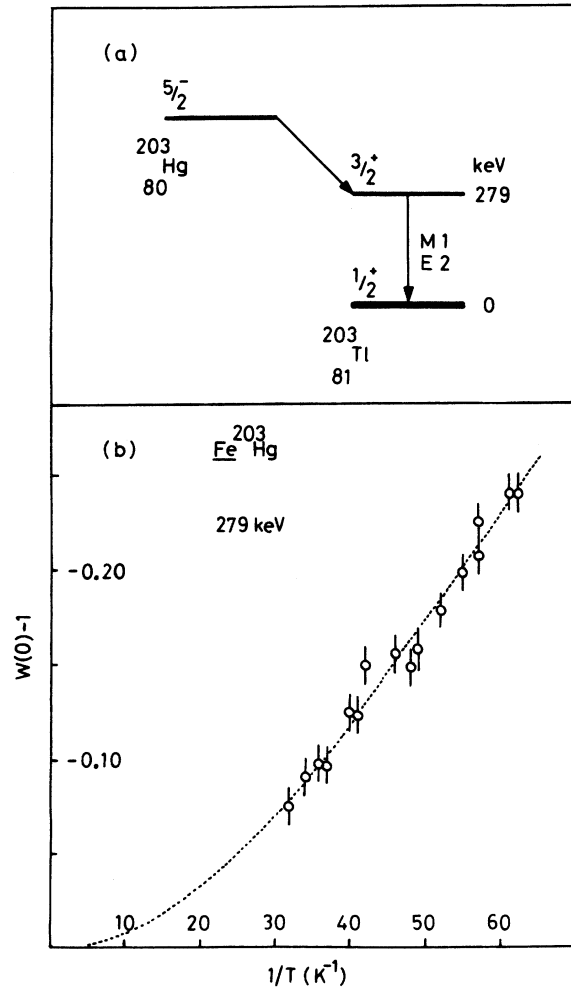


FIG. 3. (a) Decay scheme of  $^{203}\text{Hg}$ . (b) Temperature-dependent normalized axial anisotropy for the 279-keV  $\gamma$  from implanted  $^{203}\text{FeHg}$ . The dotted line is the computed curve for 100% of Hg nuclei experiencing a hyperfine field of 840 kG.

in Fig. 3(b). The dotted line through the experimental points is the calculated anisotropy for 100% of nuclei experiencing a field of 840 kG, using the measured  $E2/M1$  mixing ratio<sup>15</sup>  $\delta = +1.2(2)$  for the  $\gamma$  transition and assuming the preceding  $5/2^-$  to  $3/2^+$   $\beta$  decay to be pure  $j_\beta = 1$ . If we allow for the uncertainty in  $\delta$ , the field could be in the range 815–924 kG. If either the  $\beta$  decay involved was partly  $j_\beta = 2$  character or if less than 100% of nuclei saw the full field then the field extracted would be greater. However, the shape of the anisotropy curve provides an upper limit of 1100 kG on the field.

Thus, because of the interplay between the percentage in good sites, the decay parameters, and the hyperfine field, nuclear orientation is only able to set relatively crude limits on the hyperfine field.

### C. NMR/ON of $^{203}\text{Hg}$

In an NMR/ON experiment, resonance is observed by the detection of the change in anisotropy occurring when the populations of the  $2I + 1$  hyperfine substates are changed by resonant rf absorption. The techniques involved are described in Ref. 14. In the case of  $^{203}\text{Hg}$ ,  $\mu$  and  $I$  are known so if resonance can be observed,  $B_{\text{hf}}$  will be determined,

$$\nu_L = \mu |B_{\text{hf}} + B_{\text{app}}| / I\hbar. \quad (2)$$

For the NMR/ON experiment the sample was cooled to 13 mK, polarized in an external field of 2.1 kG, and the anisotropy of the 279-keV  $\gamma$  ray observed by a  $3 \times 3$  in. NaI(Tl) detector. The estimated field of 815–1100 kG suggested a resonance search range of 205–280 MHz. With the rf signal frequency modulated over  $\pm 400$  kHz a search in 1-MHz steps was made starting at 205 MHz. At 216 MHz a resonance was observed, its existence being confirmed by comparison of frequency-modulated (FM) and carrier-wave-alone (CW) counts. After measuring the relaxation time the resonance in Fig. 4 was plotted out, each point being calculated from the difference between CW and FM counts at the same center frequency with due allowance for warmup and sufficient time left between counts for the nuclei to relax. To obtain a lower limit on the fraction of Hg nuclei influenced by the resonant rf field, we record the integrated destruction, i. e., the summed fractional destructions of anisotropy recorded at a series of frequency settings covering the full linewidth and separated by twice the modulation range. The dotted curve is for a full width at half-maximum (FWHM) of 3.2 MHz, 60% integrated destruction of anisotropy, and a center frequency of 216.4 MHz. After allowing for the applied external field the frequency of 216.4(2) MHz gives a hyperfine field of  $-838.1(8)$

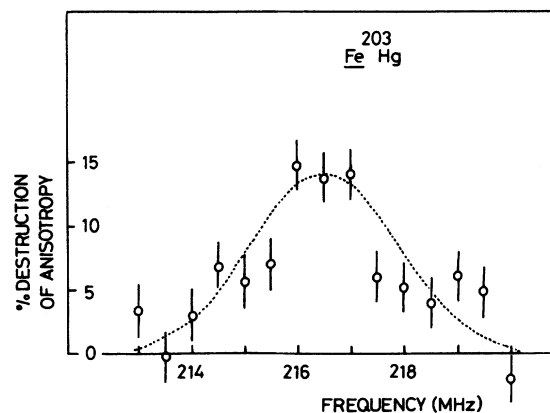


FIG. 4. NMR/ON of  $^{203}\text{Hg}$ . The dotted curve is for an integrated destruction of 60%.

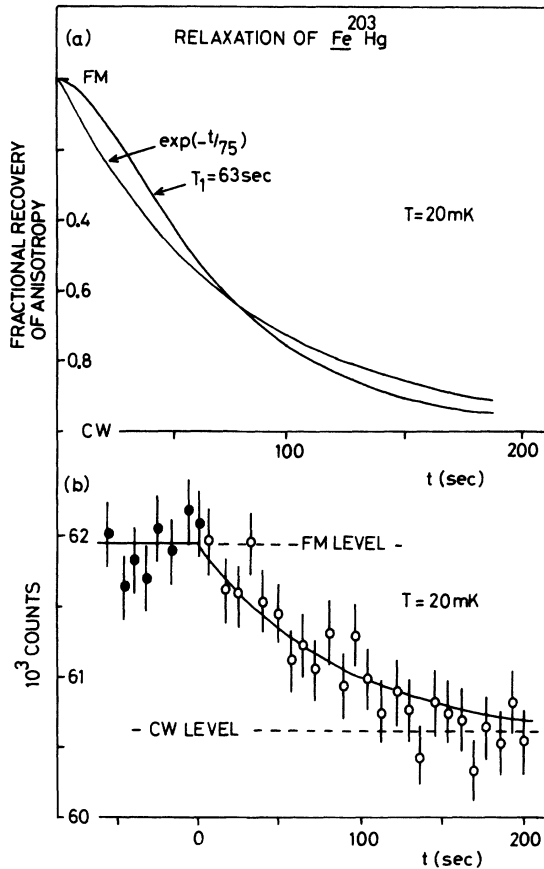


FIG. 5. Relaxation of  $^{203}\text{Hg}$  in Fe at 20 mK. (a) Comparison of single exponential curve with time constant 75 sec and full theory with  $T_1$  of 63 sec. (b) Experimental data.

kG [using  $\mu = 0.84895(13)$ ,  $I = \frac{5}{2}$ , Ref. 6 corrected for diamagnetic shielding]. Later runs at higher rf power indicated a total integrated destruction of 75(7)%.

The frequency range from 123 to 210 MHz, corresponding to 480–820 kG, was searched for other resonances. None was found at the available sensitivity; 10% of nuclei in a resonance of the same width as that at 216.4 MHz one would have been detected.

The same experiment was performed on the weaker single-crystal source; it gave the same anisotropies and resonant frequency, within experimental error. If the anisotropy data are fitted to a two-site model in which  $x\%$  of nuclei experience a hyperfine field of  $-838$  kG and the remaining  $(100-x)\%$  are in zero field, then  $x = 97(3)$ .

The single-crystal source was finally annealed at  $350^\circ\text{C}$  for 2 h in an atmosphere of dry hydrogen. It was found that half the activity was lost from the source and that which remained showed only half the normal anisotropy, presumably due to the pre-

cipitation of Hg (Ref. 16).

#### D. Spin-lattice relaxation time

The spin lattice relaxation time was measured at 20 mK by observing the recovery of anisotropy following the removal of frequency modulation of the rf field, the remaining carrier-wave field ensuring the same rf heating and hence no change in sample temperature. A center frequency of 216.5 MHz and  $\pm 400$ -kHz modulation were used and sufficient rf power applied to saturate this portion of the resonance. Counts were accumulated automatically in a multichannel analyzer operating in the multiscaler mode. Figure 5(b) shows the result of 11 relaxations, the solid line through the points being a fit to a simple exponential,  $e^{-t/\tau}$ , giving  $\tau = 75(10)$  sec.

This time  $\tau$  is useful when considering the time to allow for relaxation following an FM count. However, the time constant obtained from the single-exponential fit bears no simple relation to the properly defined  $T_1$  of the system.<sup>17</sup>

Recent work<sup>18</sup> on the adiabatic fast passage, using NMR/ON, of very dilute impurities in Fe has shown that the spin-lattice interaction is much stronger than the spin-spin one, i. e.,  $T_1 = T_2$ . Spanjaard and Hartmann-Boutron<sup>19</sup> have developed the relaxation theory applicable to such a case and derive the following expression for the rate of change of population of the  $m$ th substate:

$$\frac{dp_m}{dt} = \frac{1}{T_1(1+e^{-\beta})} \{ [I(I+1) - m(m+1)] (p_{m+1} - p_m e^{-\beta}) + [I(I+1) - m(m-1)] (p_{m-1} e^{-\beta} - p_m) \},$$

where

$$\beta = \mu B / IkT.$$

This expression can be integrated numerically from given initial conditions and then the time development of the anisotropy can be calculated. Figure 5(a) shows the recovery of anisotropy of the 284-keV  $\gamma$ -ray assuming that for a fraction  $y$  of the nuclei the substate populations at resonance saturation are equal, the remainder being unaffected. The fraction  $y$  obtained was 75(7)%. The populations of the substates are initially set equal because saturation of a NMR/ON resonance corresponds to 100% destruction of anisotropy<sup>20</sup> and when this is achieved the hyperfine substates have equal populations. Using this model of the relaxation the experimental data were fitted to give  $T_1 = 61(7)$  sec.

This value of  $T_1$  is in good agreement with the empirical formula<sup>17</sup>

$$T_1 T \gamma_N^2 B_{\text{hf}}^2 \sim 2 \times 10^{18} \text{ K sec}^{-1},$$

which predicts 53 sec.

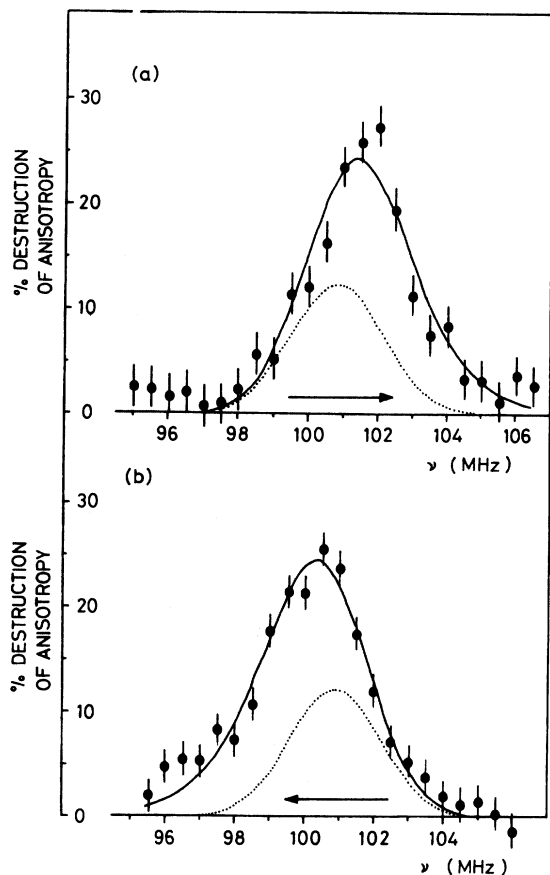


FIG. 6. NMR/ON resonances for  $Fe^{197}Hg^m$ . (a) The response obtained for increasing frequency and (b) that obtained for decreasing frequency. The dotted curve represents the intrinsic line shape; the solid lines are the fitted curves taking into account relaxation.

#### IV. HYPERFINE-INTERACTION MEASUREMENTS ON $Fe^{197}Hg^m$

##### A. Source preparation

The 23.8h activity  $^{197}Hg^m$  was produced by deuteron irradiation of gold.  $^{197}Hg^m$  was subsequently implanted into two 10- $\mu$ m-thick iron foils bought from Goodfellow Metals, England. The iron foils had previously been soldered onto copper tags. The implantation was performed at 80 keV with the Bonn mass separator. The separation of the isobaric gold and mercury isotopes was achieved through the large difference in vapor pressures of these two elements at moderate ion-source temperatures. The implantation doses were  $\sim 4 \times 10^{13}/\text{cm}^2$  and  $\sim 9 \times 10^{12}/\text{cm}^2$ , respectively. The stronger source had a maximum concentration of  $10^{-2}$  at%.

##### B. NMR/ON on $^{197}Hg^m$ in iron

The copper tags holding the samples were soldered onto the cold fingers of chrome-alum salt

pills using Wood's metal. During this procedure the iron was immersed in liquid nitrogen. The resonance runs were performed at temperatures below 20 mK in an external field of 2.3 kG. The 134-keV  $\gamma$  quanta following the decay of  $^{197}Hg^m$  (for a decay scheme see, for instance, Ref. 6) were detected by a Ge(Li) detector on the external-field axis, and the anisotropy was monitored with a single-channel analyzer. Figure 6 shows the resonance response at frequencies around 100 MHz for the strong source. The percentage destruction of anisotropy, being derived from the difference between counts taken with and without frequency modulation relative to the counting level at 1 K, is plotted (a) for increasing frequency and (b) for decreasing frequency. The difference in the two curves is due to the spin-lattice relaxation time  $T_1$  being longer than the counting interval of 100 sec per point. The solid curves represent a simultaneous fit to the up and down sweep data assuming a simple exponential recovery of anisotropy following resonance and using the experimental frequency modulation of  $\pm 400$  kHz. The dotted curves are the computed line shapes for a relaxation time much shorter than the counting period. It is interesting to note that the experimental peak destruction is larger than would have been found with fast relaxation. The fitted center frequency of the resonance is

$$\nu_L = 100.9(1) \text{ MHz.}$$

From this frequency

$$B_{\text{hf}}(FeHg) = -839.5(8) \text{ kG}$$

was calculated using the value of the magnetic moment of the  $I = \frac{13}{2}$  isomeric state of  $^{197}Hg$  [ $\mu = -1.027684(3)$ , Ref. 21 corrected for diamagnetic shielding] and allowing for the external field of 2.3 kG. The determination of the center frequency from the data is independent of assumptions as to the mechanism of the relaxation, being the centroid of the combined sweep up and down data. The line-width was found to be  $\Gamma = 1.8(1)$  MHz and the integrated destruction of anisotropy  $D = 50(3)\%$ . The relaxation-time constant is  $\tau = 227(25)$  sec at about 20 mK. Using the full relaxation theory the value of  $\tau$  observed corresponds to  $T_1 = 190(40)$  sec at about 20 mK. This value again agrees reasonably with the prediction of Eq. (4),  $T_1 = 249$  sec. The same experiment on the weaker source gave the same frequency as the strong source within experimental error.

We also searched the frequency range from 75 to 90 MHz for a possible resonance corresponding to the TDPAC result ( $\nu_L = 82$  MHz for  $B_{\text{hf}} = 680$  kG). None was found at the available sensitivity; we can put an upper limit of 10% on the percentage of nuclei with a sharp resonance frequency in this re-

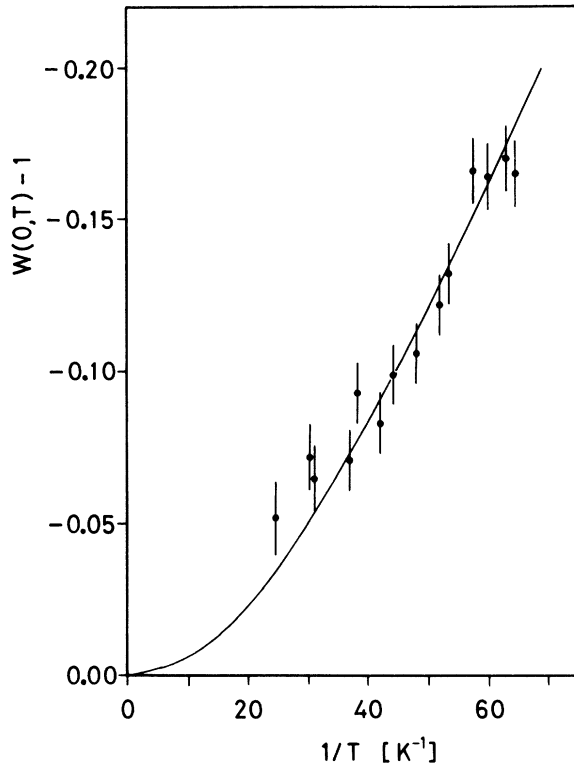


FIG. 7. Temperature-dependent anisotropy for the 134-keV  $\gamma$  line in the decay of  $^{197}\text{Hg}^m$ . The solid line is the fitted curve for 96% of nuclei experiencing a field  $B_{\text{hf}} = -839.5$  kG.

gion.

### C. Nuclear orientation of $^{197}\text{Hg}^m$

For the nuclear-orientation (NO) experiment a  $\text{Fe}^{60}\text{Co}$  thermometric source was soldered to the cold finger in addition to the strong  $^{197}\text{Hg}^m$  source. The sample was polarized in an external field of 6.7 kG. The full  $\gamma$  spectrum up to 1.4 MeV was observed with a Ge(Li) detector on the axis of orientation and stored for successive 1000-sec counting periods in a multichannel analyzer while the pill warmed from 16 mK to 1 K. In Fig. 7 the experimental anisotropies of the 134-keV line are plotted versus the reciprocal temperature.

The data were interpreted in terms of a simple two-site model. It was assumed that in one site the nuclei see the full hyperfine field found in the resonance experiment, whereas in the other site the hyperfine field is zero. A fit of the theoretical orientation function to the data is shown in Fig. 7. In it the only free parameter was the percentage of nuclei seeing the full hyperfine field, all the directional and orientation parameters being known. A value of 96(2)% in good sites was found.

## V. DISCUSSION

### A. Hyperfine field of mercury in iron

Table I lists values of  $B_{\text{hf}}(\text{FeHg})$  obtained by different experimental techniques. The present results are in excellent agreement with each other and give the field below 1 K.

All the other experiments listed in Table I were performed at room temperature. The techniques applied were time-integral PAC (IPAC) and TDPAC. The results of the IPAC experiments vary between 440 and 640 kG, whereas the two TDPAC experiments both gave a result of about 680 kG. The IPAC experiments appear to be subject to systematic errors. For example, it is very difficult to determine from the data whether all nuclei were in a site with unique hyperfine field or whether they are subject to quite a broad hyperfine-field distribution. In contrast, the TDPAC experiments allow one to observe directly a unique hyperfine interaction and the approximate proportion of nuclei subject to it. Therefore one is inclined to adopt the value from the TDPAC experiments  $B_{\text{hf}} = 680(40)$  kG (average from Refs. 5 and 6) for the hyperfine field at room temperature. Thus there appears to be a discrepancy of about 25% between the values for the field at room temperature and below 1 K. The difference is very unlikely to be due to the use of erroneous  $g$  factors since the two TDPAC experiments were performed with two different isotopes, as were the NMR/ON experiments.

We are therefore led to the hypothesis that the difference in the hyperfine fields measured at room temperature with TDPAC and below 1 K with NMR/ON should be ascribed to an anomaly in the temperature dependence. Obviously a TDPAC experiment with  $\text{FeHg}$  at different temperatures would be very valuable in confirming this hypothesis.

From the two NMR/ON results we obtain the hyperfine anomaly between the two Hg levels in the Fe lattice,  $\Delta(^{197}\text{Hg}^m - ^{203}\text{Hg}) = +0.17(14)\%$ . This value can be compared with the much more accurate value  $\Delta(^{197}\text{Hg}^m - ^{203}\text{Hg}) = +0.25(2)\%$  from hfs measurements in the Hg atom.<sup>21</sup> The small magnitude of  $\Delta$  and the resulting low precision of the measurement in Fe render any attempt to separate a contact and noncontact contribution to the Hg field in Fe from these data of little value.<sup>22</sup>

### B. Lattice location of mercury in iron

The channeling measurement indicated that over 90% of the impurity nuclei reside in substitutional sites. The integrated destruction obtained in the NMR/ON work was 75(7)% ( $\text{Fe}^{203}\text{Hg}$ ) and 50(3)% ( $\text{Fe}^{197}\text{Hg}$ ), although only in the former case was a deliberate attempt made to saturate the resonance. The lower limit for the high-field-site fraction from these data is 75%. Thus the well-

TABLE III. The results of channeling experiments on the elements Au to Bi implanted into Fe. The percentage substitutional being evaluated as  $100 \times [1 - \chi_0(\text{impurity})]/[1 - \chi_0(\text{Fe})]$ .

Impurity	Dose (cm <sup>-2</sup> )	Energy (keV)	$\chi_0$ or scan	Approximate percentage substitutional	Reference
Au	$1 \times 10^{15}$	80	$\chi_0$	88	10
Hg	$5 \times 10^{14}$	80	scan	92	this work
Tl	$2 \times 10^{14}$	170	$\chi_0$	84	23
Pb	$2 \times 10^{14}$	100	$\chi_0$	82	23
Bi	$2 \times 10^{14}$	100	$\chi_0$	79	23
	$5 \times 10^{14}$	200	scan	72 <sup>a</sup>	24

<sup>a</sup>Percent substitutional from  $\chi_0$  alone.

defined NMR/ON field is associated with the substitutional Hg site. Since lack of complete destruction of the anisotropy is the rule rather than the exception in NMR/ON experiments, the fraction in this site may exceed 75%.

The NO data, if interpreted on a simple model with nuclei experiencing either the full field or zero, are consistent with full-field fractions of 97(3)% ( $Fe^{203}Hg$ ) and 96(2)% ( $Fe^{197}Hg^m$ ). An alternative "model" fit to the NO data would be 75% in full-field sites and 25% experiencing a distribution of fields with a mean value of 710 kG but yielding no sharp resonance.

The room-temperature TDPAC work of Krien *et al.*<sup>6</sup> indicated only 50% of the Hg ions in the full-field site, the remainder in a distribution of fields. This fraction is well below the 75% NMR/ON minimum, and the possible variation of this fraction would be of interest in the study of the temperature dependence of the hyperfine interaction by TDPAC.

We note that the high substitutional fraction observed is not incompatible with the insolubility<sup>16</sup> of Hg in Fe as ion implantation results generally in a nonequilibrium situation. The instability of the substitutional site was demonstrated by the annealing results.

It is interesting to correlate the present result with the locations found for neighboring elements when implanted into Fe. Table III shows the results of channeling experiments on the elements from Au to Bi. Care, however, must be exercised in the interpretation of  $\chi_0$  measurements, additional information, either from angular scans or

from hyperfine interaction measurements being required before definite assignments to sites can be made. This is illustrated by the cases of  $FeBi$  and  $FeTl$ . A recent channelling experiment<sup>24</sup> on  $FeBi$  gave angular yields inconsistent with a simple distribution between substitutional and random sites. In order to obtain a good fit to the data, ~30% of impurities had to occupy a specific nonsubstitutional site and only ~40% of impurities were substitutional, compared with the 70% substitutional indicated by  $\chi_0$  measurements. A hyperfine interaction<sup>5</sup> experiment on implanted sources of  $FeBi$ ,  $FePb$ , and  $FeTl$  would perhaps shed some light on the nature of the nonsubstitutional sites involved.

#### ACKNOWLEDGMENTS

In connection with the location work and measurements on  $^{203}Hg$  the authors are grateful to G. Read for his help in crystal preparation, W. Temple and G. Gard of the Electromagnetic Separator Group, Harwell, for implantations, and to T. Sparrow and the operating staff of the Harwell 5-MV Van de Graaff for making the channeling experiment possible. In connection with the work on  $^{197}Hg^m$  they thank the staff of the Karlsruhe cyclotron group for performing the irradiation. Special thanks are due to R. Folle for his assistance in arranging the experiment. One of them (P. H.) wishes to thank the Deutscher Akademischer Austauschdienst for a NATO research grant and the Clarendon Laboratory for hospitality during his visit. This work was supported by grants from the Science Research Council.

\*On leave of absence from: Institut für Strahlen- und Kernphysik der Universität Bonn, Bonn, Germany.

<sup>1</sup>L. Keszthelyi, I. Berkes, I. Dezsai, B. Molnar, and L. Pocs, Phys. Lett. **8**, 195 (1964).

<sup>2</sup>J. Murray, T. A. McMath, and J. A. Cameron, Can. J. Phys. **46**, 75 (1968).

<sup>3</sup>F. C. Zawislak, D. D. Cook, and M. Levanoni, Phys.

Lett. **B 30**, 541 (1969).

<sup>4</sup>A. F. Dilmanian and R. Kalish, Phys. Rev. **B 8**, 3093 (1973).

<sup>5</sup>R. S. Raghavan, P. Raghavan, E. N. Kaufmann, K. Krien, and R. A. Naumann, Phys. Rev. **B 7**, 4132 (1973).

<sup>6</sup>K. Krien, A. G. Bibiloni, K. Freitag, J. C. Soares,



- and R. Vianden, Phys. Rev. B 8, 2248 (1973).
- <sup>7</sup>M. Kawamura and T. Tomiyama, J. Phys. Soc. Jpn. 36, 27 (1974).
- <sup>8</sup>R. L. King, C. H. Liu, and H. H. Stroke, Phys. Lett. B 31, 567 (1970).
- <sup>9</sup>N. J. McG. Tegart, *The Electrolytic and Chemical Polishing of Metals in Research and Industry*, 2nd ed. (Pergamon, London, 1959).
- <sup>10</sup>R. B. Alexander, thesis (Oxford, 1971) (unpublished); Atomic Energy Research Establishment report No. 6849, 1971.
- <sup>11</sup>K. C. Knox, Nucl. Instrum. Methods 81, 202 (1970).
- <sup>12</sup>R. B. Alexander, P. T. Callaghan, and J. M. Poate, Phys. Rev. B 9, 3022 (1974).
- <sup>13</sup>R. J. Blin-Stoyle and M. A. Grace, Hand. Phys. 42, 555 (1951).
- <sup>14</sup>N. J. Stone, At. Energy Rev. 12, 585 (1974).
- <sup>15</sup>Nuclear Data Tables 5, 531 (1971).
- <sup>16</sup>M. Hansen, *Constitution of Binary Alloys*, 2nd ed. (McGraw Hill, New York, 1958).
- <sup>17</sup>N. J. Stone, in *Hyperfine Interactions in Excited Nuclei*, edited by G. Goldring and R. Kalish (Gordon and Breach, London, 1971), p. 237.
- <sup>18</sup>P. T. Callaghan, P. D. Johnston, and N. J. Stone, J. Phys. C 7, 3161 (1974).
- <sup>19</sup>D. Spanjaard and F. Hartmann-Boutron, Solid State Commun. 8, 323 (1970).
- <sup>20</sup>D. Spanjaard and F. Hartmann-Boutron, J. Phys. (Paris) 33, 565 (1972).
- <sup>21</sup>R. J. Reimann and M. N. McDermott, Phys. Rev. C 7, 2065 (1973).
- <sup>22</sup>N. J. Stone, J. Phys. (Paris) 34, C4-69 (1973).
- <sup>23</sup>L. C. Feldman, E. N. Kaufmann, D. W. Mingay, and W. W. Augustyniak, Phys. Rev. Lett. 27, 1145 (1971).
- <sup>24</sup>P. Kittel, thesis (Oxford, 1974) (unpublished).